European Journal of Medicinal Chemistry 125 (2017) 400–410

Contents lists available at ScienceDirect

European Journal of Medicinal Chemistry

journal homepage: http://www.elsevier.com/locate/ejmech

Research paper

Design, synthesis and docking studies of novel 1,2-dihydro-4-hydroxy-2-oxoquinoline-3-carboxamide derivatives as a potential anti-proliferative agents

Saleha Banu [a], Rajitha Bollu [a], Rajashaker Bantu [a], Lingaiah Nagarapu [a, *], Sowjanya Polepalli [b], Nishant Jain [b], Radhika Vangala [c], Vijjulatha Manga [c]

[a] Organic Chemistry Division II (CPC), CSIR-Indian Institute of Chemical Technology, Tarnaka, Hyderabad, 500007, India
[b] Center for Chemical Biology, CSIR-Indian Institute of Chemical Technology, Tarnaka, Hyderabad, 500007, India
[c] Molecular Modeling and Medicinal Chemistry Group, Department of Chemistry, Osmania University, Tarnaka, Hyderabad, 500007, India

ARTICLE INFO

Article history:
Received 22 April 2016
Received in revised form
19 September 2016
Accepted 20 September 2016
Available online 21 September 2016

Keywords:
Roquinimex
1,2-dihydro-4-hydroxy-2-oxoquinoline-3-carboxamides
Piperazines
Anti-proliferative
Multiple sclerosis
Cell lines and molecular modeling

ABSTRACT

A new series of 4-hydroxy-1-methyl-2-oxo-1,2-dihydroquinoline-3-carboxamide hybrids **8a-l** have been designed and synthesized using peptide coupling agents with substituted *N*-phenyl piperazines and piperidines with good to excellent yields. The synthesized compounds were evaluated for their *in vitro* anti-proliferative activity against PANC 1, HeLa and MDA-MB-231. The compounds **8d, 8e, 8f, 8g, 8h** and **8k** exhibited considerable anti-proliferative activity with GI_{50} values ranging from **0.15** to **1.4** μM. The structure and anti-proliferative activity relationship was further supported by *in silico* molecular docking study of the active compounds against tubulin protein.

1. Introduction

Quinolines and their hetero fused scaffolds are prevalent molecular structures in chemistry, biology and medicine [1–3]. Among the various types of substituted quinolines, 1,2-dihydro-4-hydroxy-2-oxoquinoline-3-carboxamide derivatives gained specific importance as privileged medicinal scaffolds (Fig. 1). For example, Roquinimex (Linomide) (A), a novel immuno modulator, has been shown to be effective against various types of cancers [4,5]and autoimmune diseases such as MRL/l mice [6], (NZB_NZW) F1 hybrid mice [7] and experimental autoimmune encephalomyelitis [8,9]. Recent clinical trials suggest that (A) has potential in the treatment of autoimmune disease such as rheumatoid arthritis, systemic lupus erythematosis and multiple sclerosis [10–12]. Interestingly, Tasquinimod (B) is a lead second generation quinoline-3-carboxamide linomide analogue which is anti-angiogenic agent for the treatment of prostate cancer, which produces robust and consistent *in vivo* growth inhibition as well as suppression of metastasis in a large series of pre-clinical human xenograft and rodent prostate cancer models [13,14]. Laquinimod (C) is an oral drug in clinical trials for the treatment of multiple sclerosis (MS) which was developed by Active Biotech Research AB with linomide as a lead compound [15,16] and has successfully undergone a clinical phase II trial as multiple sclerosis medication [17]. Owing to the importance of these scaffolds, synthesis and functionalization of 1,2-dihydro-4-hydroxy-2-oxoquinoline-3-carboxamide compounds attract great interest.

Literature survey informs that piperazines and substituted piperazines are important family of heterocyclic compounds as they have attracted significant interest in medicinal chemistry [18–20] and also some piperidine derivatives are important due to their antimicrobial properties [21]. Many currently notable drugs contain a piperazine ring as a part of their molecular structure as shown in Fig. 2.

The molecular manipulation of promising lead compounds is still a major line of approach to develop new drugs. It involves an effort to combine the separate pharmacophoric groups of similar

* Corresponding author.

http://dx.doi.org/10.1016/j.ejmech.2016.09.062
0223-5234/

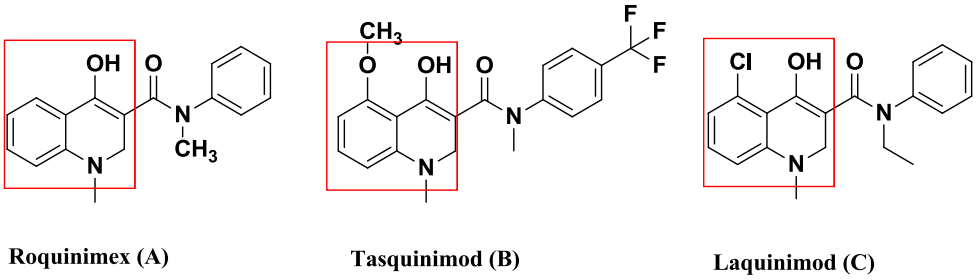

Fig. 1. Structure of Roquinimex and roquinimex based under clinical trial cancer therapy agents.

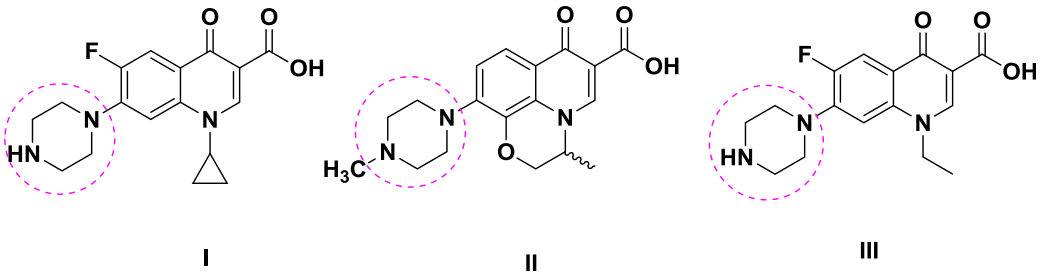

Fig. 2. Representative examples of biologically active piperazinyl substituted quinoline derivatives.

activity into one compound, thus making structural changes in the biological activity. Considering the above facts, it was thought worthwhile to synthesize the compounds with a view to obtain certain chemical entities with active pharmacophores in a single molecular frame work [22–24].

As a part of our endeavor towards new and efficient anticancer agents [25], we herein report an efficient method for the synthesis of novel 4-hydroxy-1-methyl-2-oxo-*N*-(3-oxo-3-(piperdine/piperazin-1-yl)propyl)-1,2-dihydroquinoline-3-carboxamide hybrids **8a-l** in good to excellent yields. The synthesized hybrids **8a-l** were evaluated for their *in vitro* anti-proliferative activity against three human cancer cell lines such as PANC 1 (pancreatic), HeLa (cervical) and MDA-MB-231 (breast) using a SRB cell proliferation assay to estimate the viability or growth. Significantly, the compounds **8d, 8e** and **8k** showed promising anti-proliferative activity with GI_{50} values ranging from **0.15** to **1.4** μM, **0.30–0.94** μM and **0.51–1.3** μM respectively against all three human cancer cell lines. The structure and anti-proliferative activity relationship was further supported by *in silico* molecular docking study of the active compounds against tubulin protein. Numerous molecules were reported as tubulin polymerization inhibitors where some of them were quinoline derivatives [26–28].

2. Results and discussion

2.1. Chemistry

The synthesis of the desired 4-hydroxy-1-methyl-2-oxo-*N*-(3-oxo-3-(piperdine/piperazin-1-yl)propyl)-1,2-dihydroquinoline-3-carboxamideswas performed in six steps starting from isatoic anhydride using diethyl malonate and β-alanine ester.

The first synthetic step involved the subsequent *N*-methylation of isatoic anhydride with iodomethane in presence of sodium hydride in DMF about 5 h at room temperature to give the corresponding *N*-methylated isatoic anhydride (**2**). The corresponding *N*-methylated isatoic anhydride was then condensed with diethyl malonate in presence of sodium hydride at 120 °C in DMF solution for 12 h and refluxed to get the compound, ethyl 4-hydroxy-1-methyl-2-oxo-1,2-dihydroquinoline-3-carboxylate (**3**), which was further hydrolysed in presence of glacial acetic acid and hydrochloric acid at 85 °C for 4 h to get the targeted compound, 4-hydroxy-1-methyl-2-oxo-1,2-dihydroquinoline-3-carboxylic acid (**4**), in quantitative yield (Scheme 1).

Treatment of 1,2-dihydroquinoline-3-carboxylic acid with β-alanine ester in the presence of HOBt, EDC.HCl and triethylamine at room temperature for 16 h gave ethyl 3-(4-hydroxy-1-methyl-2-oxo-1,2-dihydroquinoline-3-carboxamido)propanoate (**5**), which was further hydrolysed using KOH, ethanol at reflux temperature for 4 h to get 3-(4-hydroxy-1-methyl-2-oxo-1,2-dihydroquinoline-3-carboxamido)propanoic acid (**6**). Treatment of compound **6** with substituted piperazines and secondary amines (**7a-l**) in the presence of HOBT, EDC.HCl and triethyl amine at room temperature for 24 h gave the targeted 4-hydroxy-1-methyl-2-oxo-*N*-(3-oxo-3-(piperdine/piperazin-1-yl)propyl)-1,2-dihydroquinoline-3-carboxamides **8a-l** in good yields (Scheme 2) (Table 1).

The synthesized 1,2-dihydroquinoline-3-carboxamides **8a-l** were subjected to analytical characterization and confirmed on the basis of their spectral data. In ^{1}H NMR spectra, the characteristic triplet signals appeared for piperazine protons at δ 3.10–3.85 ppm. The structures for all these compounds were further confirmed by HRMS analysis. For instance, **8a** displayed a molecular ion peak at *m/z*453.19246$[M+H]^+$ suggesting the molecular formula of $C_{24}H_{25}O_4N_4F$.Additionally, the IR spectra for the target compounds **8a-l** exhibited characteristic absorption bands at 1629-1633 cm^{-1},3060-3300 cm^{-1} and 2853-2952 cm^{-1} which corresponded to C=O, N–H and C–H_3 respectively.

2.2. 2Pharmacological evaluation

2.2.1. 1Effects of the compounds on the viability of human cancer cells

The *in vitro* anti-proliferative activity of the designed compounds **8a-l** were evaluated against a panel of three different human cancer cell lines, PANC 1 (pancreatic), HeLa (cervical) and MDA-MB-231 (breast) summarized in Table 2. The compounds were picked for an advanced assay against these three human

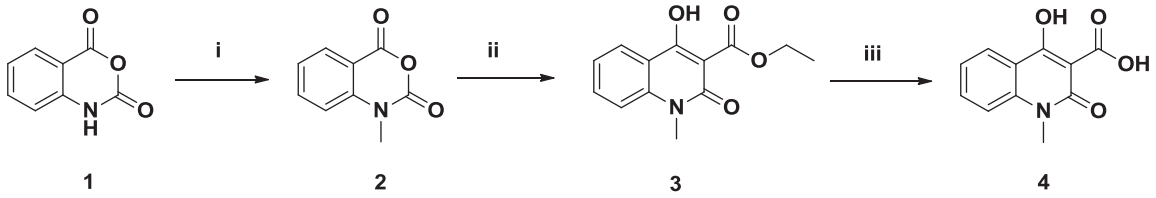

Reagents and conditions: i) CH_3I, NaH, DMF, 5 h, ii) Diethyl malonate, NaH, DMF, 120 °C, reflux, 12 h, iii) CH_3CO_2H, HCl, CH_3CH_2OH, 60 °C, 4 h, reflux.

Scheme 1. Synthesis of4-hydroxy-1-methyl-2-oxo-1, 2-dihydroquinoline-3-carboxylicacid (**4**). **X** = **a**) N-Ph-2F; **b**) N-Ph; **c**) N-Ph-4CF_3;**d**) CH_2; **e**) N-Ph-4NO_2;**f**) N–CH_2CH_3;**g**) N–CH_2-Ph; **h**) N–CH_2–2OCH_3; **i**) S; **j**) N–CH_3; **k**) N–CH_2–2OCH_3; **l**) CH_2–CH_2- Ph. ***Reagents and conditions***: i) *β*-Alanine ethyl ester HCl. EDC. HCl, HOBT, ET_3N, DCM, rt, 16 h ii) 1N KOH, ethanol, 80 °C, reflux, 4 h iii) EDC. HCl, HOBT, DCM, rt, 24 h.

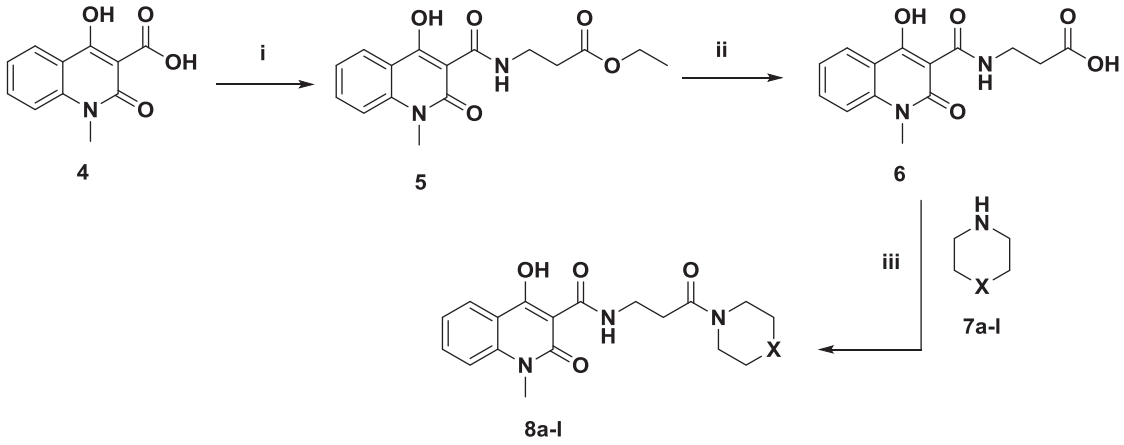

X = a) N-Ph-2F; b) N-Ph; c) N-Ph-4CF_3; d) CH_2; e) N-Ph-4NO_2; f) N-CH_2CH_3; g) N-CH_2-Ph; h) N-CH_2-2OCH_3; i) S; j) N-CH_3; k) N-CH_2-2OCH_3; l) CH_2-CH_2- Ph

Reagents and conditions: i) *β*-Alanine ethyl ester HCl. EDC. HCl, HOBT, ET_3N, DCM, rt, 16 h ii) 1N KOH, ethanol, 80 °C, reflux, 4 h iii) EDC. HCl, HOBT, DCM, rt, 24 h.

Scheme 2. Synthesis of 4-hydroxy-1-methyl-2-oxo-*N*-(3-oxo-3-piperazinyl) propyl)-1,2-dihydroquinoline-3-carboxamide hybrids (**8a-l**).

cancer cell lines at five different concentrations (0.01, 0.1, 1, 10, 100 μM). GI_{50} (growth inhibitory activity) was calculated and these values corresponded to the concentration of the compound causing 50% decrease in the net cell growth as compared to the standard drugs, Nocodazole and Combretastatin. Results were calculated for each of these parameters if the level of activity was reached; however, if the effect was not achieved, the value was expressed as greater or less than the maximum or minimum concentration tested.

Based on Table 2, the synthesized compounds **8a-l** showed significant to moderate cancer cell growth inhibition with GI_{50} values ranging from **0.15** to **5.4** μM. The effect of various substituent's attached to 1,2-dihydroquinoline-3-carboxamido propanoic acid (**6**) was examined. In particular, the compounds **8d, 8e, 8f, 8g, 8h** and **8k** showed promising anti-proliferative activity with GI_{50} values ranging from **0.15**–**1.40** μM respectively, against the three human cancer cell lines. Among them, compounds **8d, 8e** and **8k** showed good anti-proliferative activity against all the three human cancer cell lines.

The biological assessment results against PANC 1 (pancreatic) cell line indicated that the piperdine analogue **8d** exhibited good anti-proliferative activity against this particular cell line. When the activities of *N*-alkyl piperazines and *N*-phenyl piperazines were compared, the analogue **8e** with nitro group incorporated into the 4th position of phenyl ring of piperazine moiety attached to (**6**) contributed promising anti-proliferative activity against all three cell lines. The compound **8e** showed significant anti-proliferative activity against MDA-MB231. According to the data of biological research regarding the potency of the phenyl substituted compounds, the presence of nitro and methoxy groups to the phenyl ring of piperazine moiety with (**6**) displayed promising anti-proliferative activity against all the three cancer cell lines.

Moreover we noticed that the compounds **8h** and **8k** displayed similar results against all the three cell lines indicating there was no significant change in their activities due to the changes in position of the methoxy functional groups in the phenyl ring of piperazine moiety. The halogenated piperazine bearing analogues also showed considerable anti-proliferative activity against all the human cancer cell lines. The results showed that the substitutions on the ring attached to 1,2-dihdroquinoline-3-carboxamido propanoic acid have influence on the potency of anti-proliferative activity against all the three cancer cell lines. Fig. 3.

2.2.2. Molecular docking studies

Microtubules are the key components of the cytoskeleton of eukaryotic cells and has an important role in various cellular

Table 1
4-hydroxy-1-methyl-2-oxo-*N*-(3-oxo-3-(piperazinyl) propyl)-1, 2-dihydroquinoline-3-carboxamide hybrids **8(a–l)**.

Entry	Compound	2° amine	Product	yield[a]
a	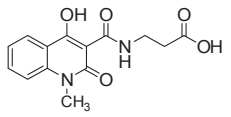	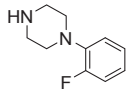	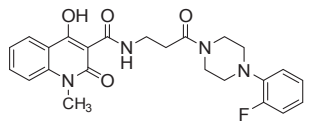	82
b	6	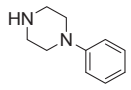	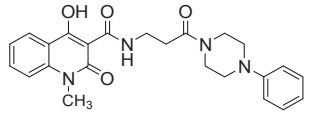	84
c	6	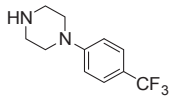	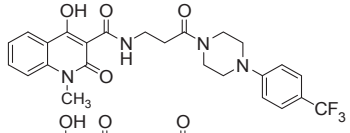	80
d	6		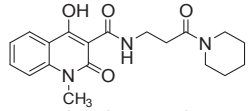	78
e	6	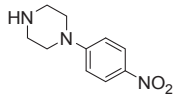	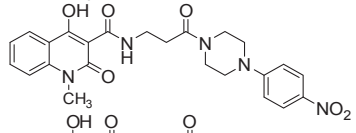	77
f	6	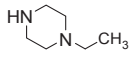	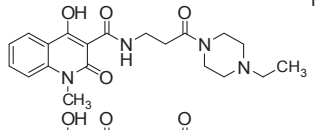	83
g	6	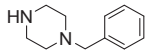	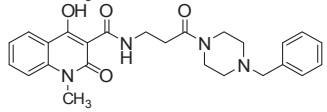	80
h	6	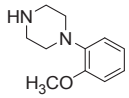	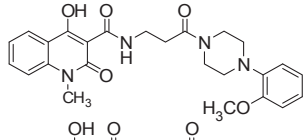	76
i	6		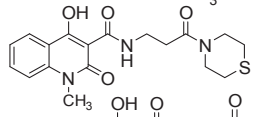	68
j	6	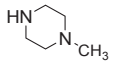	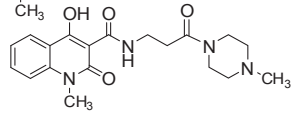	79
k	6	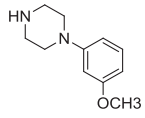	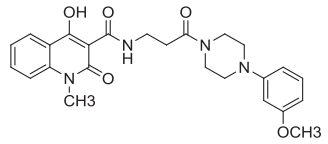	74
l	6	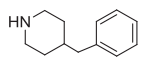	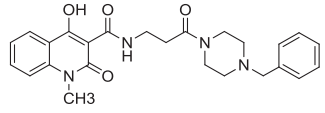	77

[a]Percentage yields of isolated products

functions such as intracellular migration and transport, cell shape maintenance, polarity, cell signalling and mitosis. It plays a critical role in cell division by involving in the movement and attachment of the chromosomes during various stages of mitosis. Therefore, microtubule dynamics is an important target for the developing anti-cancer drugs.

Combretastatin is a natural phenol that specifically binds to cochicine binding site of tubulin for its anti-mitotic effects. Based on the literature evidence the quinolines and dihydroquinolines have been reported as tubulin inhibitors. Hence in the present

Table 2
(GI_{50})[a] values of the tested compounds against three human cancer cell lines.

S.No	PANC 1	HeLa	MDA-MB-231
8a	2.5 ± 0.09	0.96 ± 0.03	1.7 ± 0.03
8b	1.57 ± 0.04	3.9 ± 0.09	1.62 ± 0.08
8c	2.55 ± 0.04	3.7 ± 0.06	5.4 ± 0.17
8d	0.15 ± 0.02	0.82 ± 0.03	1.4 ± 0.05
8e	0.42 ± 0.01	0.94 ± 0.02	0.3 ± 0.02
8f	0.48 ± 0.03	0.88 ± 0.04	1.32 ± 0.16
8g	0.95 ± 0.01	0.76 ± 0.02	0.51 ± 0.01
8h	0.7 ± 0.01	0.74 ± 0.01	1.2 ± 0.06
8i	1.91 ± 0.06	3.0 ± 0.19	2.25 ± 0.03
8j	1.66 ± 0.04	1.16 ± 0.04	0.59 ± 0.02
8k	0.51 ± 0.01	0.73 ± 0.02	1.3 ± 0.05
8l	0.68 ± 0.03	1.4 ± 0.06	0.71 ± 0.01
Nocodazole[b]	<0.01	<0.01	<0.01
Combretastatin[b]	0.059 ± 0.002	0.083 ± 0.001	0.09 ± 0.01

[a] GI_{50}: 50% Growth inhibition, concentration of drug (in μM) resulting in a 50% reduction in net protein increase compared with control cells.
[b] Positive controls.

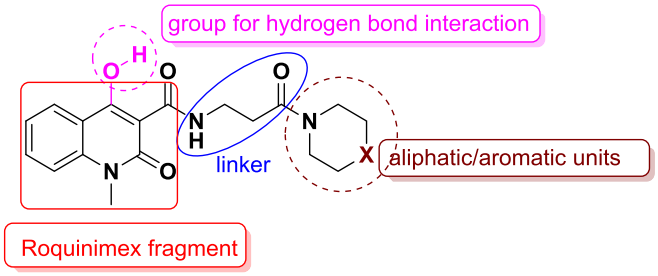

Fig. 3. Design strategy for new 4-hydroxy-1-methyl-2-oxo-*N*-(3-oxo-3-piperazinyl) propyl)-1, 2-dihydroquinoline-3-carboxamide hybrids. ***Reagents and conditions***: i) CH_3I, NaH, DMF,5 h ii) Diethyl malonate, NaH, DMF, 120 °C, reflux, 12 h iii) CH_3CO_2H, HCl, CH_3CH_2OH, 60 °C, 4 h, reflux.

study we have docked the current series of compounds along with the combretastatin in the tubulin protein to understand the probable binding mode and key active site interactions.

From the docking studies we observed that combretastatin showed hydrogen bond interactions with Val 238 and Ala 317 and hydrophobic interactions with Ala 250, Leu 255, Ala 316 and Lys 352 residues. The compounds **8d** showed hydrophobic interactions with Val 238, Leu 242, Leu 252, Lys 254, Leu 255 and Lys 352 and **8e** showed hydrophobic interactions with Val 238, Leu 242, Leu 255, Ala 316, Lys 352 and Ileu 378 residues. Fig. 4 represents the docked poses of combretastatin, **8d** and **8e** molecules in the tubulin active site. The GI_{50} and pGI_{50} values, and dock scores were given in Table 3.

From the above results we have observed that the most potent compounds **8d** and **8e** showed some common interactions (Val 238, Leu 255, Lys 352) as compared to combretastatin which is in agreement with experimental anti-proliferative activities. The other compounds also showed comparable binding and good dock scores. To validate the correlation between anti-proliferative activity and the dock score a regression analysis was performed. The correlation between experimental activity and dock scores is greater than 50% [29]. Dock score (glide score) and GI_{50} of PANC1, HeLa and MDA-MB-231 gave a correlation coefficient values (r) of −0.58, −0.52 and −0.52 which shows significant relation between biological activity and docking. The scatter plots of pGI_{50} of PANC1, HeLa, MDA-MB-231 and their dock scores are shown in Fig. 5.

Experimental molecular 3D structures of ligands checked for their ADME properties using QikProp4.0. (Table 4). ADME describes

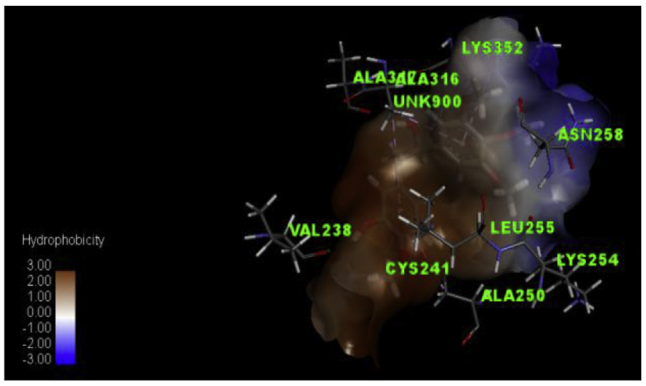

(a)

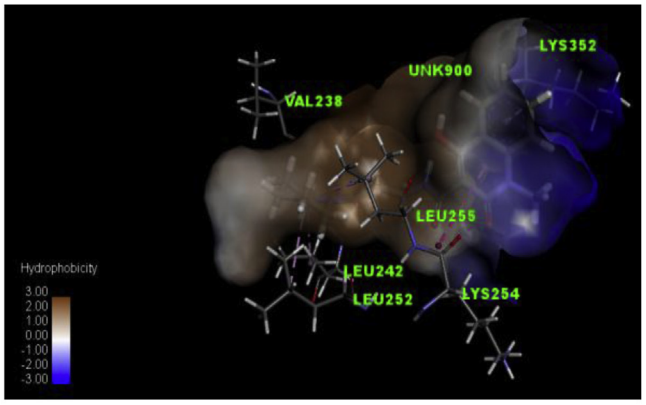

(b)

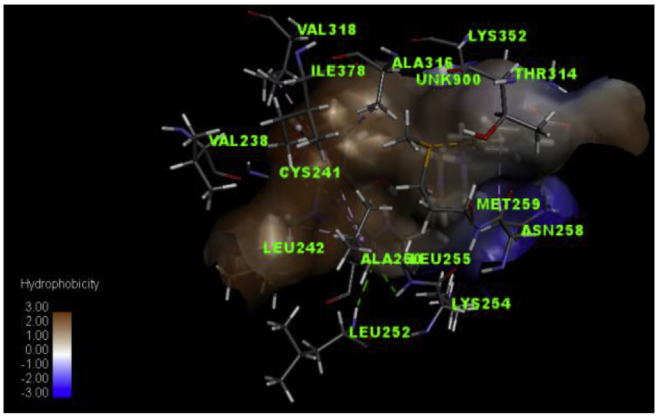

(c)

Fig. 4. a,b,c represents the dock poses of Combretastatin, **8d** and **8e** molecules in the tubulin active site.

about Absorption, Distribution, Metabolism and Excretion of drug candidates. These are considered as drug like properties need to fulfil by the drug molecule to pass through phase-I clinical trials.

They are defined as.

Absorption (A): Process of entering the drug substance into the blood stream.

in silico parameters supported are logS and logP.

Table 3
Molecules with their activities and dock scores.

Compd.	PANC 1		HeLa		MDA-MB-231		Dock score(XP)
	GI_{50}	pGI_{50}	GI_{50}	pGI_{50}	GI_{50}	pGI_{50}	
8a	2.5 ± 0.09	5.6020	0.96 ± 0.03	6.0177	1.7 ± 0.03	5.7695	−4.854
8b	1.57 ± 0.04	5.8041	3.9 ± 0.09	5.4089	1.62 ± 0.08	5.7904	−4.041
8c	2.55 ± 0.04	5.5934	3.7 ± 0.06	5.4317	5.4 ± 0.1	5.2676	−4.508
8d	0.15 ± 0.02	6.8239	0.82 ± 0.03	6.0861	1.4 ± 0.05	5.8538	−5.734
8e	0.42 ± 0.01	6.3767	0.94 ± 0.02	6.0268	0.3 ± 0.02	6.5228	−5.709
8f	0.48 ± 0.03	6.3187	0.88 ± 0.04	6.0555	1.32 ± 0.16	5.8794	−4.161
8g	0.95 ± 0.01	6.0222	0.76 ± 0.02	6.1191	0.51 ± 0.01	6.2924	−5.085
8h	0.7 ± 0.01	6.1549	0.74 ± 0.01	6.1307	1.2 ± 0.06	5.9208	−5.376
8i	1.91 ± 0.06	5.7189	3.0 ± 0.19	5.5228	2.25 ± 0.03	5.6478	−5.410
8j	1.66 ± 0.04	5.7798	1.16 ± 0.04	5.9355	0.59 ± 0.02	6.2291	−2.649
8k	0.51 ± 0.01	6.2924	0.73 ± 0.02	6.1366	1.3 ± 0.05	5.8860	−5.1
8l	0.68 ± 0.03	6.1674	1.4 ± 0.06	5.8538	0.71 ± 0.01	6.1487	−4.073
Combretastatin	0.059 ± 0.0002	7.2291	0.083 ± 0.001	7.0809	0.09 ± 0.01	7.0457	−6.793
Nocodazole	<0.01	–	<0.01	–	<0.01	–	−5.753

Distribution (D): Dispersion of drug to other parts of the body defined by logBB.

Metabolism (M): Biotransformation, irreversible transformation of parent compounds into active metabolites.

Excretion (E): Removal of drug metabolites from the body.

QikProp helps in analyzing pharmacokinetics and pharmacodynamics of the ligand by accessing drug like properties. It predicts both physically significant descriptors and pharmaceutically relevant properties. Neutralized analogues of molecules are used for calculating ADME properties. Properties consists of principal descriptors and the physiochemical properties with a detailed analysis of the predicted octanol/water partition coefficient (QPlogPo/w) and water solubility (QPlogS), critical for estimating the absorption and distribution of drugs within the body. % human oral absorption in intestine, predicted brain/blood partition coefficient (QPlogBB), predicted apparent Caco-2 cell permeability in nm/sec (QPPCaco) and predicted apparent MDCK cell permeability in nm/sec (QPPMDCK). Caco-2 cells are a model for the gut-blood barrier whereas MDCK cells are considered to be a good mimic for the blood-brain barrier. It also evaluates an acceptability of the analogues based on the Lipinski's rule of 5 (number of violations of Lipinski's rule of five) that is essential for rational drug design. Poor absorption or permeation are more likely when a ligand molecule violates Lipinski's rule of five i.e., more than 5 hydrogen bond donors, the molecular weight over 750, the log P over 5 and the sum of N's and O's over 10.

The calculated values for the synthesized molecules ranged within the acceptable limits.

Crossing the blood-brain barrier (BBB), which is a prerequisite for the entry of drugs to CNS, was found to be in the acceptable range indicating that the compounds may be considered for further development. The predicted percentage human oral absorption for all the molecules also in acceptable range.

3. Conclusion

Taken together, we synthesized a series of novel 4-hydroxy-1-methyl-2-oxo-*N*-(3-oxo-3-(piperazin-1-yl) propyl)-1,2-dihydroquinoline-3-carboxamides **8a-l** in good yields and performed anti-proliferative activity against three different human cancer cell lines, namely PANC 1, HeLa, and MDA-MB-231 (pancreatic, cervical and breast respectively). Among the tested cancer cell lines, Compounds **8d, 8e, 8f, 8g, 8h,** and **8k** exhibited promising anti-proliferative activity with GI_{50} values ranging from **0.15** to **1.4** μM against all cell lines, like PANC 1, HeLa and MDA-MB-231. Significantly, the compounds **8d** showed significant activity against PANC 1with GI_{50} value **0.15** μM, **8e** showed significant activity against MDA-MB-231 with GI_{50} value **0.30** μM and **8k** showed significant activity against HeLa with GI_{50} value **0.73** μM. Based on the biological assay, molecular docking and ADME studies, the synthesized molecules can be considered as promising lead molecules for the development of new anti cancer agents.

4. Experimental protocols

4.1. Biological study

4.1.1. Materials and methods. Cell cultures, maintenance and anti proliferative evaluation

The cell lines, PANC 1, HeLa, and MDA MB 231 (pancreatic, cervical and breast) used in this study was procured from American Type Culture Collection (ATCC), USA. The synthesized test compounds were evaluated for their *in vitro* anti-proliferative activity in these three different human cancer cell lines. A protocol of 48 h continuous drug exposure was used and an SRB cell proliferation assay was used to estimate cell viability or growth. All the cell lines were grown in Dulbecco's modified Eagle's medium (containing 10% FBS in a humidified atmosphere of 5% CO_2 at 37 °C). Cells were trypsinized when sub-confluent from T25 flasks/60 mm dishes and seeded in 96-well plates in 100 μL aliquots at plating densities depending on the doubling time of individual cell lines. The microtitre plates were incubated at 37 °C, 5% CO_2, 95% air, and 100% relative humidity for 24 h prior to the addition of experimental drugs and were incubated for 48 h with different doses (0.01, 0.1, 1, 10, 100 μM) of the prepared derivatives. After incubation at 37 °C for 48 h, the cell monolayers were fixed by the addition of 10% (wt/vol) cold trichloroacetic acid and incubated at 4 °C for 1 h and were then stained with 0.057% SRB dissolved in 1% acetic acid for 30 min at room temperature. Unbound SRB was washed with 1% acetic acid. The protein–bound dye was dissolved in 10 mM Tris base solution for OD determination at 510 nm using a microplate reader (Enspire, Perkin Elmer, USA). Using the seven absorbance measurements [time zero, (Tz), control growth, (C), and test growth in the presence of drug at the five concentration levels (Ti)], the percentage growth was calculated at each of the drug concentrations levels. Percentage growth inhibition was calculated as:

$[(Ti\text{-}Tz)/(C\text{-}Tz)] \times 100$ for concentrations for which $Ti >/= Tz$.
$[(Ti\text{-}Tz)/Tz] \times 100$ for concentrations for which $Ti < Tz$.

The dose response parameter, growth inhibition of 50% (GI_{50}) was calculated from $[(Ti\text{-}Tz)/(C\text{-}Tz)] \times 100 = 50$, which is the drug

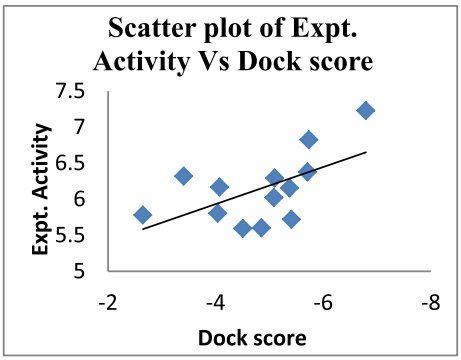

(a)

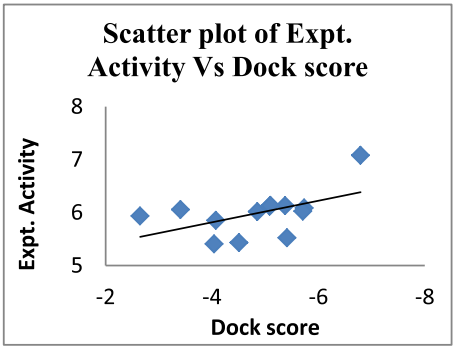

(b)

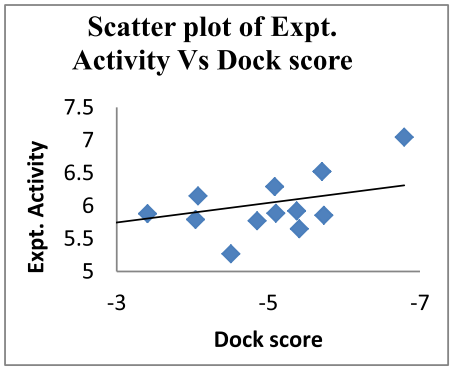

(c)

Fig. 5. Scatter plots of Experimental pGI_{50} VS Dock score values Activity 1 (PANC1) (a), Activity 2 (HeLa) (b) and Activity 3 (MDA-MB-231) (c).

concentration resulting in a 50% reduction in the net protein increase (as measured by SRB staining) in control cells during the drug incubation. Values were calculated for this parameter if the level of activity is reached; however, if the effect is not reached or is exceeded, the value for that parameter was expressed as greater or less than the maximum or minimum concentration tested.

4.2. Molecular modeling

Docking studies: Molecular docking studies were carried out using Glide version 5.6 [30]. Crystal structure of β-tubulin (PDB ID: 1SA0) [31] was downloaded from protein data bank. 12 molecules were docked into 1SA0. The hydrogen atoms were added and unwanted water molecules were removed from the protein structure. The receptor binding site was defined as a Glide enclosing box in the centroid of the co-crystallized ligand molecule and the size was set to a default value of 26 Å without any hydrogen bonding constraint.

Ligand preparation: LigPrep [32] was used to attach hydrogen, converts 2D structures to 3D, generates stereoisomer and optionally neutralizes charged structures or determines the most probable ionization state at user-defined pH. All the structures were ionized at neutral pH 7. Conformers for each ligand were generated using ConfGen by applying OPLS-2005 force field method [33].

4.3. General information

All the solvents and reagents were purchased from commercial suppliers and were used without further purification. Melting points were measured with a Fischer-Johns melting point apparatus and were uncorrected. Nuclear Magnetic Resonance spectra were recorded on 300 (Bruker) and 500 MHz (Varian) spectrometers in appropriate solvents using TMS as internal standard or the solvent signals as secondary standards and the chemical shifts are represented in δ scales. Multiplicities of NMR signals are designated as s (singlet), d (doublet), doublet of doublet (dd), t (triplet), m (multiplet, for unresolved lines), etc. ^{13}C NMR spectra were recorded on 75 and 125 MHz spectrometer. IR spectra were recorded on Perkin-Elmer model 683 or 1310 spectrometers with sodium chloride optics or KBr pellets with neat. ESI-MS were recorded on Thermo Finnigan LCQ ion trap mass spectrometer equipped with electron spray ionization. High-resolution mass spectra were obtained by using ESI-QTOF mass spectrometer. All the experiments were monitored by analytical thin layer chromatography (TLC) performed on silica gel GF_{254} pre-coated plates. After elution, the plate was visualized for the spots on TLC plates which was achieved either by exposure to UV (254 nm) light, iodine vapour and/or by dipping the plates in phosphomolybdic acid-ceric (IV) sulfate-sulfuric acid solution (PMA solution) and heating the plates at 110 °C.Solvents were removed under vacuum and heated in a water bath at 40 °C. Silica gel (60–120 mesh) was used for column chromatography. Columns were packed as the slurry of silica gel in hexane and equilibrated with the appropriate solvent/solvent mixture prior to use. The compounds were loaded neat or as a concentrated solution using the appropriate solvent system. Appropriate names (if possible) for all the new compounds were given with the help of ChemBioOffice v12.0; 2012.

4.4. Synthesis of 1-methyl-1H-benzo[d] [1,3] oxazine-2, 4-dione (2)

Isatoic anhydride (12.26 mmol) in DMF (30 mL) was taken, sodium hydride (18.3 mmol) was added portion wise and stirred for 10 min. Reaction mixture was cooled to 0 °C, Iodomethane (18.3 mmol) was added drop wise and stirred at RT for 5 h. Reaction was monitored by TLC. After completion of reaction, ice water was added, extracted with ethyl acetate. Organic layer was dried over anhydrous sodium sulfate and evaporated to dryness. Crude product was purified by column chromatography using an eluent of 35% ethyl acetate in hexane to afford 1 -methyl- l *H*-benzo[*d*][l,3] oxazine-2,4-dione as brown coloured solid with 64% yield.^{1}HNMR (400 MHz, DMSO-d_6): δ 3.59 (s, 3H, CH_3), 7.30–7.39 (m, 1 H, Ar–H), 7.79–7.86 (m, 1 H, Ar–H), 8.08–8.13(m, 1H, Ar–H).

4.5. Synthesis of ethyl 4-hydroxy-1-methyl-2-oxo-1,2-dihydroquinoline-3-carboxylate (3)

A solution of diethyl malonate (51 mmol) was added slowly to a suspension of sodium hydride (60% in mineral oil, 56 mmol) in dimethylformamide under N_2 atmosphere. The mixture was stirred

Table 4
Pharmacokinetic properties of molecules.

Compd.[a]	QPlogPo/w[b]	QPlogS[c]	QPlogBB[d]	QPPCaco[e]	QPPMDCK[f]	%Human oral absorption[g]
8a	3.792	−4.077	−0.729	454.113	564.204	96.704
8b	4.128	−4.803	−0.611	843.169	796.743	100
8c	4.723	−5.556	−0.57	462.949	1869.451	100
8d	3.05	−4.106	−0.837	548.13	464.888	93.827
8e	3.55	−6.14	−2.053	93.559	57.006	83.012
8f	2.168	−2.723	−0.576	137.328	98.524	77.902
8g	3.583	−4.433	−0.673	157.245	113.883	87.241
8h	4.294	−5.806	−1.08	464.425	406.092	100
8i	3.031	−4.027	−0.657	631.118	928.994	94.811
8j	1.819	−1.47	−0.106	243.423	216.776	80.308
8k	4.264	−5.747	−1.082	454.509	402.52	100
8l	5.21	−6.391	−0.899	771.018	625.161	96.168
Combretastatin	3.327	−3.842	−0.654	2087.011	1095.768	100

[a] Molecules.
[b] Predicted octanol/water partition coefficient log P (Acceptable range−2.0 to 6.5).
[c] Predicted aqueous solubility's in mol/L (Acceptable range −6.5 to 0.5).
[d] Predicted BBB permeability (Acceptable range−3 to 1.2).
[e] Predicted Caco cell permeability in nm/s (Acceptable range:< 25 is poor and >500 is great).
[f] Predicted apparent MDCK cell permeability in nm/s (Acceptable range in nm/s (Acceptable range: <25 is poor and>500 is great).
[g] Percentage of human oral absorption (Acceptable range: <25 is poor and >80% is high).

at room temperature until the evolution of hydrogen gas ceased, then heated to 90 °C for 30 min and cooled to room temperature. A solution of *N*-methylisatoic anhydride (56 mmol) in dimethylformamide was added slowly and the mixture was heated overnight at 120 °C. The mixture was then cooled to room temperature, poured into ice water, and acidified by cold 10% HCl. The solids formed were filtered and washed several times by water to afford ethyl 4-hydroxy-1-methyl-2-oxo-1, 2-dihydroquinoline-3-carboxylate as light brown coloured solid with 78% yield.^{1}H NMR (500 MHz, $CDCl_3$): δ1.49 (t,J = 7.1 Hz, 3H, CH_3),3.66 (s, 3H, CH_3), 4.51 (q, J = 7.1 Hz, 2H, CH_2), 7.27–7.38 (m, 1H, Ar–H), 7.66–7.73 (m, 1H, Ar–H), 8.19 (dd, J = 7.9 Hz, 1.5 Hz, 1H, Ar–H), 14.20 (s, 1H, OH).

4.6. Synthesis of 4-hydroxy-1-methyl-2-oxo-1,2-dihydroquinoline-3-carboxylic acid (4)

1,2-Dihydro-4-hydroxy-*l*-methyl-2-oxo-3-quinoline carboxylic acid methyl ester (3.61 mmol) was added to glacial acetic acid (88.6 mmol) at 25–30 °C followed by the addition of hydrochloric acid (54.5 mmol) and then heated to 80–85 °C. The reaction mixture was stirred at 80–85 °C for 6 h. The resulting mass was cooled to 10–15 °C followed by the addition of ethanol (10 mL). The resulting solid was filtered and washed with ethanol (10 mL) and then dried to get l,2-dihydro-4-hydroxy-*l*-methyl-2-oxo-3- quinoline carboxylic acid as white coloured solid with 86% yield. ^{1}H NMR (500 MHz, $CDCl_3$): δ3.77 (s, 3H, CH_3), 7.38–7.54 (m, 2H, Ar–H), 7.77–7.87 (m, 1H,Ar–H), 8.27 (dd,, J = 8.0 Hz, 1.2 Hz, 1H, Ar–H), 14.55 (s, 1H, COOH), 15.60 (s, 1H,OH).

4.7. Synthesis of ethyl 3-(4-hydroxy-1-methyl-2-oxo-1,2-dihydroquinoline-3-carboxamido) propanoate (5)

Compound **4** (1 mmol) was dissolved in freshly distilled dichloromethane (5 mL) under nitrogen atmosphere. Then HOBt (1.1 mmol), EDC.HCl (1.1 mmol) were added to it. The reaction mixture was stirred for 5 min, and β-alanine ethyl ester hydrochloride (1.5 mmol) was added slowly, followed by the addition of triethylamine (2 mmol) and stirred for 16 h at room temperature. The progress of the reaction was monitored by TLC. After completion of the reaction, water (10 mL) was added to the reaction mixture and extracted with dichloromethane. Organic layer was collected and dried over anhydrous Na_2SO_4. Solvent was removed under reduced pressure and the resultant compound was recrystallized with ether to afford the title compound **5** as pale brown solid with 76% yield.^{1}H NMR (500 MHz, $CDCl_3$): 1.29 (t, J = 7.1 Hz, 3H, CH_3) 2.67 (t, J = 6.5 Hz, 2H, CH_2), 3.68 (s, 3H, CH_3), 3.74 (q, J = 6.4 Hz, 2H, CH_2), 4.20 (q, J = 7.1 Hz, 2H, CH_2), 7.28–7.33 (m, 1H, Ar–H), 7.34–7.38 (m, 1H, Ar–H), 7.65–7.72 (m, 1H, Ar–H), 8.21 (dd, J = 8.0 Hz, 1.5 Hz, 1H), 10.59 (t, J = 6.7 Hz, 1H, CONH).

4.8. Synthesis of 3-(4-hydroxy-1-methyl-2-oxo-1,2-dihydroquinoline-3-carboxamido) propanoic acid (6)

The compound **5** (1.2 mmol) was dissolved in ethanol (10 mL), added 1*N* potassium hydroxide solution (10 mL) and the reaction mixture was refluxed for 4 h, and completion of the reaction was monitored by TLC. After completion of the reaction, the reaction mixture was allowed to cool to room temperature, neutralized with diluted hydrochloric acid and the solid separated was filtered through Buckner funnel and washed with water and dried over reduced pressure to obtain the crude compound. The above crude product was recrystallized from ethanol to obtain the title compound **6** as white solid with 74% yield. ^{1}H NMR (300 MHz, $CDCl_3$): 2.75 (t, J = 6.4 Hz, 2H, CH_2), 3.69 (s, 3H, CH_3), 3.72–3.80 (m, 2H, CH_2), 7.30–7.38 (m, 2H, Ar–H), 7.65–7.73 (m, 1H, Ar–H), 8.23 (dd, J = 7.7 Hz,1.37 Hz, 1H, Ar–H), 10.62 (t, J = 5.6 Hz, 1H, CONH).^{13}C NMR (75 MHz, $CDCl_3$): δ20.07, 32.69, 34.95, 96.71, 114.09, 122.17, 125.36, 133.55, 162.50, 139.83, 162.50, 170.99, 179.50; MS (ESI): m/z 291$[M+H]^+$;

4.9. 9General procedure for the synthesis of compounds8a-l

Compound **6** (1 mmol) was dissolved in freshly distilled dichloromethane (5 mL) under nitrogen atmosphere. Then HOBt (1.1 mmol), EDC,HCl (1.1 mmol) were added to it. The reaction mixture was stirred for 5 min, secondary amine **7a-l** (1.2 mmol) was added in a slow stream and followed by the addition of triethylamine (2 mmol) and the reaction mixture was stirred for 24 h at room temperature. The progress of the reaction was monitored by TLC. After completion of the reaction, water (10 mL) was added to the reaction mixture and extracted with dichloromethane. Organic layer was collected and dried over anhydrous Na_2SO_4. After filtration, the solvent was removed under reduced pressure and the crude product was purified by silica gel chromatography using an

eluent of 50% ethyl acetate in hexane.

4.9.1. N-(3-(4-(2-fluorophenyl)piperazin-1-yl)-3-oxopropyl)-4-hydroxy-1-methyl-2-oxo-1,2-dihydroquinoline-3-carboxamide (8a)

Light brown solid (82% yield): m.p: 160–164 °C; IR (KBr, ν): 3090, 2924, 2854, 1633, 1574, 1504, 1442, 1231, 1021, 803,764 cm^{-1}; ^1H NMR (500 MHz, $CDCl_3$): δ2.73 (t, $J = 6.4$ Hz, 2H, CH_2), 3.04–3.09 (m, 4H, $2CH_2$), 3.64 (t, $J = 5.2$ Hz, 2H, CH_2), 3.68 (s, 3H, CH_3), 3.78–3.82 (m, 2H, CH_2), 3.82–3.85 (m, 2H,CH_2), 6.89–6.99 (m, 2H, Ar–H), 7.01–7.07 (m, 2H, Ar–H), 7.28–7.33 (m, 1H, Ar–H), 7.34–7.37 (m, 1H, Ar–H), 7.67–7.71 (m, 1H, Ar–H), 8.22 (dd, $J = 8.0$ Hz, 1.3 Hz, 1H, Ar–H), 10.64 (t, $J = 5.5$ Hz, 1H, CONH); ^{13}C NMR (75 MHz, $CDCl_3$): δ29.65, 32.77, 45.50, 50.33, 50.78, 96.83, 114.16, 116.07, 119.14, 122.25, 123.06, 124.46, 133.66, 139.93, 162.51, 169.38, 171.11, 171.81; MS (ESI):*m/z* 453 $[M+H]^+$; HRMS: Calcd for $C_{24}H_{25}O_4N_4F$: 453.19326, Found: 453.19246.

4.9.2. 4-Hydroxy-1-methyl-2-oxo-N-(3-oxo-3-(4-phenylpiperazin-1-yl)propyl)-1,2-dihydroquinoline-3-carboxamide (8b)

Light brown solid (84% yield): m.p:162–166 °C; IR (KBr, ν): 3379, 2925, 2858, 1634, 1494, 1441, 1230, 1020, 803, 764 cm^{-1}; ^1H NMR (500 MHz, $CDCl_3$): δ 2.73 (t, $J = 6.4$ Hz, 2H, CH_2), 3.17 (t, $J = 5.1$ Hz, 4H, $2CH_2$), 3.63 (t, $J = 5.1$ Hz, 2H, CH_2), 3.66 (s, 3H, CH_3), 3.77–3.86 (m, 4H, $2CH_2$), 6.88–6.96 (m, 4H, Ar–H), 7.28–7.36 (m, 3H, Ar–H), 7.66–7.70 (m, 1H, Ar–H), 8.22 (dd, $J = 8.0$ Hz, 1.5 Hz, 1H, Ar–H), 10.63 (t, $J = 5.7$ Hz, 1H, CONH); ^{13}C NMR (125 MHz, $CDCl_3$): δ 29.13, 32.76, 35.02, 45.29, 49.36, 96.83, 114.17, 116.59, 120.49, 122.24, 125.44, 129.16, 133.65, 139.91, 150.85, 169.38, 171.11, 171.79. (ESI):*m/z* 435 $[M+H]^+$; HRMS: Calcd for $C_{24}H_{26}O_4N_4$: 435.20268, Found: 435.20198.

4.9.3. 4-Hydroxy-1-methyl-2-oxo-N-(3-oxo-3-(4-(4-(trifluoromethyl)phenyl)piperazin-1-yl)propyl)-1,2-dihydroquinoline-3-carboxamide (8c)

White solid (80% yield)): m.p:134–137 °C; IR (KBr, ν): 3101, 2924, 2855, 1633, 1574, 1408, 1338, 1155, 1098, 1072,765 cm^{-1}; ^1H NMR (500 MHz, $CDCl_3$): δ 2.73 (t, $J = 6.4$ Hz, 2H, CH_2), 3.27 (t, $J = 5.1$ Hz, 4H, $2CH_2$), 3.64 (s, 3H, CH_3), 3.65–3.68 (m, 2H, CH_2), 3.78–3.84 (m, 4H, $2CH_2$), 6.90 (d, $J = 8.6$ Hz, 2H, Ar–H), 7.28–7.35 (m, 2H, Ar–H), 7.44–7.49 (m, 2H, Ar–H), 7.66–7.70 (m, 1H, Ar–H), 8.21 (dd, $J = 8.1$ Hz, 1.5 Hz, 1H, Ar–H), 10.62 (t, $J = 5.4$ Hz, 1H, CONH); ^{13}C NMR (75 MHz, $CDCl_3$): δ29.16, 32.77, 35.01, 41.67, 45.50, 50.31, 96.83, 114.17, 116.06, 119.13, 122.26, 123.17, 125.45, 133.65, 162.50, 169.37, 171.10, 171.80; MS (ESI): *m/z* 503$[M+H]^+$; HRMS: Calcd for $C_{25}H_{25}O_4N_4F_3$: 503.19007, Found: 503.19005.

4.9.4. 4-Hydroxy-1-methyl-2-oxo-N-(3-oxo-3-(piperidin-1-yl) propyl)-1,2-dihydroquinoline-3-carboxamide (8d)

Pale yellow solid (78% yield)): m.p:148–152 °C; IR (KBr, ν): 3422, 2926, 2853, 1633, 1567, 1445, 1411, 1337, 1252, 1015, 763 cm^{-1}; ^1H NMR (500 MHz, $CDCl_3$): δ 1.52–1.58 (m, 4H, $2CH_2$), 1.61–1.65 (m, 2H, CH_2), 2.66 (t, $J = 6.6$ Hz, 2H, CH_2), 3.39 (t, $J = 5.3$ Hz, 2H, CH_2), 3.59 (t, $J = 5.4$ Hz, 2H, CH_2), 3.68 (s, 3H, CH_3), 3.77 (q, $J = 6.4$ Hz, 2H, CH_2), 7.27–7.32 (m, 1H, Ar–H), 7.33–7.37 (m, 1H, Ar–H), 7.65–7.70 (m, 1H, Ar–H), 8.21 (dd, $J = 7.9$ Hz, 1.5 Hz, 1H, Ar–H), 10.60 (t, $J = 6.5$ Hz, 1H, CONH); ^{13}C NMR (75 MHz, $CDCl_3$): δ25.42, 26.32, 29.64, 32.81, 35.08, 42.62, 46.36, 96.17, 114.14, 122.18, 125.44, 133.59, 162.50, 168.96, 171.81; MS (ESI): *m/z* 358$[M+H]^+$; HRMS: Calcd for $C_{19}H_{23}O_4N_3$: 358.17613, Found:358.17672.

4.9.5. 4-Hydroxy-1-methyl-N-(3-(4-(4-nitrophenyl)piperazin-1-yl)-3-oxopropyl)-2-oxo-1,2-dihydroquinoline-3-carboxamide (8e)

Red solid (77% yield)): m.p:169–173 °C; IR (KBr, ν): 3249, 2925, 2854, 1725, 1633, 1595, 1307, 1112, 1020, 751 cm^{-1}; ^1H NMR (500 MHz, $CDCl_3$): δ 2.74 (t, $J = 6.4$ Hz, 2H, CH_2), 3.42–3.49 (m, 4H, $2CH_2$), 3.65 (s, 3H, CH_3), 3.66–3.71 (m, 2H, CH_2), 3.81 (q, $J = 6.4$ Hz, 2H, CH_2), 3.85 (t, $J = 5.4$ Hz, 2H, CH_2), 6.78–6.82 (m, 2H, Ar–H), 7.29–7.36 (m, 2H, Ar–H), 7.67–7.71 (m, 1H, Ar–H), 8.09–8.13 (m, 2H, Ar–H), 8.21 (dd, $J = 7.9$ Hz, 1.3 Hz, 1H, Ar–H), 10.63 (t, $J = 5.3$ Hz, 1H, CONH); ^{13}C NMR (75 MHz, $CDCl_3$): δ29.10, 32.75, 35.04, 41.21, 44.97, 48.01, 77.31, 76.99, 76.67, 96.81, 114.90, 114.17, 122.27, 125.43, 126.44, 133.70, 139.91, 152.81, 171.80, 162.48, 171.15, 169.49; MS (ESI): *m/z* 480$[M+H]^+$; HRMS: Calcd for $C_{24}H_{25}O_6N_5$: 480.18776, Found: 480.18926.

4.9.6. N-(3-(4-ethylpiperazin-1-yl)-3-oxopropyl)-4-hydroxy-1-methyl-2-oxo-1,2-dihydroquinoline-3-carboxamide (8f)

Light brown solid (83% yield)): m.p:165–170 °C; IR (KBr, ν): 3564, 3240, 2925, 2853, 1633, 1584, 1339, 1231, 1097, 956, 747 cm^{-1}; ^1H NMR (300 MHz, $CDCl_3$): δ 1.03 (t, $J = 7.1$ Hz, 3H, CH_3), 2.41–2.44 (m, 6H, $3CH_2$), 2.67 (t, $J = 6.4$ Hz, 2H, CH_2), 3.48 (t, $J = 4.8$ Hz, 2H, CH_2), 3.67–3.69 (m, 5H, CH_3, CH_2), 3.74–3.79 (m, 2H, CH_2), 7.29–7.36 (m, 2H, Ar–H), 7.66–7.70 (m, 1H, Ar–H), 8.21 (dd, $J = 7.9$ Hz, 1.2 Hz, 1H, Ar–H), 10.62 (t, $J = 5.1$ Hz, 1H, CONH); ^{13}C NMR (75 MHz, $CDCl_3$): δ11.77, 29.58, 32.69, 34.95, 41.46, 45.23, 52.10, 52.72, 96.71, 114.09, 122.17, 125.36, 133.55, 139.83, 162.47, 169.14, 170.99; MS (ESI): *m/z* 387$[M+H]^+$; HRMS: Calcd for $C_{20}H_{26}O_4N_4$: 387.20268, Found: 387.20369.

4.9.7. N-(3-(4-benzylpiperazin-1-yl)-3-oxopropyl)-4-hydroxy-1-methyl-2-oxo-1,2-dihydroquinoline-3-carboxamide (8g)

Brown solid (80% yield)): m.p:172–177 °C; IR (KBr, ν): 3425, 3076, 2924, 2853, 1638, 1568, 1458, 1336, 1214, 1082, 954, 751 cm^{-1}; ^1H NMR (500 MHz, $CDCl_3$): δ 2.41–2.45 (m, 4H, $2CH_2$), 2.63–2.68 (m, 2H, CH_2), 3.14–3.19 (m, 2H, CH_2), 3.46 (t, $J = 5.0$ Hz, 2H, CH_2), 3.64–3.69 (m, 5H, CH_3, CH_2), 3.76 (q, $J = 6.4$ Hz, 2H, CH_2), 7.29–7.37 (m, 7H, Ar–H), 7.64–7.72 (m, 1H, Ar–H), 8.21 (dd, $J = 8.1$ Hz, 1.3 Hz, 1H, Ar–H), 10.62 (t, $J = 5.9$ Hz, 1H, CONH); ^{13}C NMR (75 MHz, $CDCl_3$): δ29.15, 34.98, 45.24, 50.10, 52.59, 62.78, 96.65, 114.16, 122.24, 125.43, 127.25, 128.27, 129.11, 133.62, 137.33, 160.74, 169.22, 171.03; MS (ESI): *m/z* 449$[M+H]^+$; HRMS: Calcd for $C_{25}H_{28}O_4N_4$: 449.21833, Found: 449.21891.

4.9.8. 4-Hydroxy-N-(3-(4-(2-methoxyphenyl)piperazin-1-yl)-3-oxopropyl)-1-methyl-2-oxo-1,2-dihydroquinoline-3-carboxamide (8h)

Light brownsolid (76% yield): m.p:162–164 °C; IR (KBr, ν): 3251, 2925, 2855, 1629, 1589, 1499, 1335,1273, 1024, 751 cm^{-1}; ^1H NMR (300 MHz, $CDCl_3$): δ 2.73 (t, $J = 6.4$ Hz, 2H, CH_2), 2.99–3.08 (m, 4H, $2CH_2$), 3.61–3.65 (m, 2H, CH_2), 3.66 (s, 3H, CH_3), 3.76–3.81 (m, 2H, CH_2), 3.83–3.86 (m, 2H, CH_2), 3.87 (s, 3H, CH_3), 6.85–6.91 (m, 3H, Ar–H), 6.98–7.05 (m, 1H, Ar–H), 7.28–7.36 (m, 2H, Ar–H), 7.64–7.77 (m, 1H, Ar–H), 8.20 (dd, $J = 7.9$ Hz, 1.1 Hz, 1H, Ar–H), 10.63 (t, $J = 5.6$ Hz, 1H, CONH); ^{13}C NMR (125 MHz, $CDCl_3$): δ 29.15, 32.76, 35.08, 45.65, 50.53, 55.39, 96.86, 111.20, 114.16, 118.36, 120.96, 122.24, 123.50, 125.46, 133.63, 140.57, 152.18, 169.31, 171.11, 171.82; MS(ESI): *m/z* 465$[M+H]^+$; HRMS: Calcd for $C_{25}H_{28}O_5N_4$: 465.21325, Found: 465.21294.

4.9.9. 4-Hydroxy-1-methyl-2-oxo-N-(3-oxo-3-thiomorpholinopropyl)-1,2-dihydroquinoline-3-carboxamide (8i)

Brown liquid (68% yield)): IR (KBr, ν): 3247, 2925, 2814, 1634, 1567, 1454, 1209, 1145, 1004, 747 cm^{-1}; ^1H NMR (500 MHz, $CDCl_3$):δ 2.31–2.54 (m, 4H, $2CH_2$), 2.67 (t, $J = 6.4$ Hz, 2H, CH_2), 3.65–3.67 (m, 4H, $2CH_2$), 3.68 (s, 3H, CH_3), 3.78 (q, $J = 6.25$, 2H, CH_2), 7.28–7.41 (m, 2H, Ar–H), 7.59–7.73 (m, 1H, Ar–H), 8.18–8.30 (m, 1H, Ar–H), 10.62 (t, $J = 5.3$ Hz,1H, CONH); ^{13}C NMR (125 MHz, $CDCl_3$): δ26.38, 29.70, 32.87, 35.14, 42.67, 96.23, 114.20, 122.24, 125.50, 133.64, 162.56, 169.02, 171.87; MS (ESI): *m/z* 376$[M+H]^+$; HRMS: Calcd for $C_{18}H_{21}O_4N_3S$: 376.13255, Found: 376.13316.

4.9.10. 4-Hydroxy-1-methyl-N-(3-(4-methylpiperazin-1-yl)-3-oxopropyl)-2-oxo-1,2-dihydroquinoline-3-carboxamide (8j)

Light brown liquid (79% yield); IR (KBr, ν): 3235, 2930, 2796, 1632, 1563, 1504, 1445, 1337, 1144, 1002, 762 cm^{-1}; ^1H NMR (500 MHz,$CDCl_3$): δ2.29 (s, 3H, CH_3), 2.36–2.41 (m, 4H, $2CH_2$), 2.67 (t, J = 6.4 Hz, 2H, CH_2), 3.48 (t, J = 5.0 Hz, 2H, CH_2), 3.64–3.70 (m, 5H, CH_3, CH_2), 3.75–3.79 (m, 2H, CH_2), 7.28–7.36 (m, 2H, Ar–H), 7.68 (t, J = 7.6 Hz, 1H, Ar–H), 8.19–8.22 (m, 1H, Ar–H), 10.60 (t, J = 6.1 Hz, 1H, CONH); ^{13}C NMR (75 MHz, $CDCl_3$): δ29.15, 32.76, 35.02, 96.84, 114.16, 122.25, 125.46, 133.62, 139.93, 162.52, 169.21, 171.08; MS (ESI): m/z373$[M+H]^+$; HRMS: Calcd for $C_{19}H_{24}O_4N_4$: 373.18703, Found: 373.18598.

4.9.11. 4-Hydroxy-N-(3-(4-(3-methoxyphenyl)piperazin-1-yl)-3-oxopropyl)-1-methyl-2-oxo-1,2-dihydroquinoline-3-carboxamide (8k)

Light brown solid (74% yield): m.p:165–168 °C; IR (KBr, ν): 3446, 3084, 2923, 2856, 1633, 1571, 1496, 1438, 1335, 1227, 1017, 927, 763, 695 cm^{-1}; ^1H NMR (500 MHz, $CDCl_3$): δ2.72 (t,J = 6.4 Hz, 2H, CH_2), 3.14–3.18 (m, 4H, $2CH_2$), 3.60–3.64 (m, 2H, CH_2),3.66 (s, 3H, CH_3), 3.78 (s, 3H, CH_3), 3.79–3.81 (m, 4H, $2CH_2$), 6.43–6.48 (m, 2H, Ar–H), 7.14–7.22 (m, 2H, Ar–H), 7.27–7.36 (m, 2H, Ar–H), 7.66–7.71 (m, 1H, Ar–H), 8.21 (dd, J = 8.0 Hz, 1.5 Hz, 1H, Ar–H), 10.62 (t, J = 5.8 Hz, 1H, CONH);^{13}C NMR (75 MHz, $CDCl_3$): δ32.79, 35.05, 41.48, 45.25, 49.30, 55.18, 96.85, 103.06, 105.52, 109.26, 114.18, 122.27, 125.48, 129.89, 133.66, 160.56, 169.42, 171.84; MS (ESI): m/z 465 $[M+H]^+$; HRMS: Cacld for $C_{25}H_{28}O_5N_4$: 465.21325, Found: 465.21077.

4.9.12. N-(3-(4-benzylpiperidin-1-yl)-3-oxopropyl)-4-hydroxy-1-methyl-2-oxo-1,2-dihydroquinoline-3-carboxamide (8l)

Light yellow solid (77% yield); m.p: 154–158 °C; IR (KBr, ν): 3247, 2925, 2854, 1724, 1638, 1284, 1110,746 cm^{-1}; ^1H NMR (500 MHz,$CDCl_3$): δ1.14–1.26 (m, 4H, $2CH_2$), 1.72–1.77 (m, 1H, CH), 2.52–2.58 (m, 2H, CH_2), 2.63–2.66 (m, 2H, CH_2), 3.66 (s, 3H, CH_3), 3.70–3.83 (m, 6H, $3CH_2$), 7.08–7.12 (m, 2H, Ar–H), 7.17–7.21 (m, 1H, Ar–H), 7.23–7.25 (m, 1H, Ar–H), 7.27–7.31 (m, 2H, Ar–H), 7.33–7.36 (m, 1H, Ar–H), 7.62–7.70 (m, 1H, Ar–H), 8.18–8.22 (m, 1H, Ar–H), 10.59 (t, J = 5.8 Hz, 1H, CONH); ^{13}C NMR (75 MHz, $CDCl_3$): δ29.12, 32.38, 38.16, 41.97, 42.89, 45.63, 96.83, 114.13, 125.42, 125.97, 128.22, 128.99, 133.59, 139.87, 162.48, 169.00, 171.02, 171.80; MS (ESI): m/z 449 $[M+H]^+$; HRMS: Calcd for $C_{26}H_{30}N_3O_4$: 448.22068, Found: 448.22275.

Acknowledgements

The authors gratefully acknowledge the financial support through the project: **DST-SERB/EMEQ-078/2013**andthe University grant commission (UGC) (23/12/2012(II)EU-V), New Delhi for the award of fellowship to **SB**.

Appendix A. Supplementary data

Supplementary data related to this article can be found at http://dx.doi.org/10.1016/j.ejmech.2016.09.062.

References

[1] A.K. El-Damasy, S.H. Seo, N.C. Cho, S.B. Kang, A.N. Pae, K.S. Kim, G. Keum, Design, synthesis, *in-vitro* antiproliferative activity and kinase profile of new picolinamide based 2-amido and ureido quinoline derivatives, Eur. J. Med. Chem. 101 (2015) 754–768.

[2] V. Spano, B. Parrino, A. Carbone, A. Montalbano, A. Salvador, P. Brun, D. Vedaldi, P. Diana, G. Cirrincione, P. Barraja, Pyrazolo[3,4-h] quinolines promising photosensitizing agentsin the treatment of cancer, Eur. J. Med. Chem. 102 (2015) 334–351.

[3] I. Briguglio, R. Loddo, E. Laurini, M. Fermeglia, S. Piras, P. Corona, P. Giunchedi, E. Gavini, G. Sanna, G. Giliberti, C. Ibba, P. Farci, P.L. Colla, S. Pricl, A. Carta.Synthesis, cytotoxicity and antiviral evaluation of new series of imidazo[4,5-g]quinoline and pyrido[2,3-g] quinoxalinone derivatives, Eur. J. Med. Chem. 105 (2015) 63–79.

[4] T. Kalland, Effects of the immunomodulator Ls 2616 on growth and metastasis of the murine B16-F10 melanoma, Cancer Res. 46 (1986) 3018–3022.

[5] T. Ichikawa, J.C. Lamba, P.I. Christensson, B. Hartley-Asp, The antitumor effects of the quinoline-3-carboxamide linomide on dunning R-3327 rat prostatic cancers, Cancer Res. 52 (1992) 3022–3028.

[6] A. Tarkowski, K. Gunnarsson, L.-A. Nilson, L. Lindholm, T. Stalhandske, Succesfull Treatment of Autoimmunity in MRL/1 mice with LS-2616, a new immunomodulator, Arthr. Rheum. 29 (1986) 1405. T. Kalland, Effects of the Immunomodulator Ls 2616 on Growth and Metastasis of the Murine B16-F10 Melanoma, Cancer Res. 46(1986) 3018-3022.

[7] A. Tarkowski, K. Gunnarsson, T. Stalhandske, Effects of LS-2616 administration upon the autoimmune disease (NZBXNZW) F1 hybrid mice, Immunology 59 (1986) 589–594.

[8] D.M. Karussis, D. Lehmann, S. Salvin, U. Vourka-Karussis, R. Mizrachi-Koll, H. Ovadia, T. Kalland, O. Abramsky, Treatment of Chronic-relapsing experimental autoimmune encephalomyelitics with the synthetic immunomodulator linomide, Proc. Natl. Acad. Sci. U.S.A. 90 (1993) 6400–6404.

[9] D.M. Karussis, D. Lehmann, S. Salvin, U. Vourka-Karussis, R. Mizrachi-Koll, H. Ovadia, D. Ben-Num, T. Kalland, O. Abramsky, Inhibition of acute, experimental autoimmune encephalomyelitis by the synthetic immunomodulator linomide, Ann. Neurol. 34 (1993) 654–660.

[10] O. Andersen, J. Lycke, P.O. Tollesson, A. Svenningsson, B. Runmarker, A.S. Linde, M. Astrom, P. Gjorstrup, S. Ekholm, Linomide reduces the rate of active lesions in relapsing-remitting multiple sclerosis, Mult. Scler. 1 (1996) 348.

[11] O. Andersen, J. Lycke, P.O. Tollesson, A. Svenningsson, B. Runmarker, A.S. Linde, M. Astrom, P. Gjorstrup, S. Ekholm, Linomide reduces the rate of active lesions in relapsing-remitting multiple sclerosis, Neurology 47 (1996) 895–900.

[12] D.M. Karussis, Z. Meiner, D. Lehmann, J.M. Gomori, A. Schwarz, A. Linde, O. Abramsky, Treatment of secondary progressive multiple sclerosis with the immunomodulator linomide: a double-blind, placebo controlled pilot study with monthly magnetic resonance imaging evaluation, Neurology 47 (1996) 341–346.

[13] J.T. Isaacs, R. Pili, D.Z. Qian, S.L. Dalrymple, J.B. Garrison, N. Kyprianou, A. Björk, A. Olsson, T. Leanderson, Identification of ABR-215050 as lead secondgeneration quinoline-3-carboxamide anti-angiogenic agent for the treatment of prostate cancer, Prostate 66 (2006) 1768–1778.

[14] J.T. Isaacs, L. Antony, S.L. Dalrymple, W.N. Brennen, S. Gerber, H. Hammers, et al., Tasquinimod is an allosteric modulator of HDAC4 survival signaling within the compromised cancer microenvironment, Cancer Res. 73 (2013) 1386–1399.

[15] J.H. Noseworthy, J.S. Wolinsky, F.D. Lublin, Linomide in relapsing and secondary progressive MS: part I: trial design and clinical results, North Am. Linomide investigators,Neurology 54 (2000) 1726–1733.

[16] S. Jönsson, G. Andersson, T. Fex, T. Fristedt, G. Hedlund, K. Jansson, L. Abramo, I. Fritzson, O. Pekarski, A. Runström, H. Sandin, I. Thuvesson, A. Björk, Synthesis and biological evaluation of new 1,2-dihydro-4-hydroxy-2-oxo-3-quinoline carboxamides for treatment of autoimmune disorders: structure-activity relationship, J. Med. Chem. 47 (2004) 2075–2088.

[17] C. Polman, F. Barkhof, M. Sandberg-Wollheim, A. Linde, O. Nordle, T. Nederman, Treatment with laquinimod reduces development of active MRI lesions in relapsing MS, Neurology 64 (2005) 987–991.

[18] R.J. Kerns, M.J. Rybak, G.W. Kaatz, F. Vaka, R. Cha, R.G. Grucz, V.U. Diwadkar, Structural features of piperazinyl-linked ciprofloxacin dimers required foractivity against drug-resistant strains of Staphylococcus aureus, Bioorg.Med. Chem.Lett. 13 (2003) 2109–2112.

[19] A. Ryckebusch, R. Deprez-Poulain, L. Maes, M.A. Debreu-Fontaine, E. Mouray, P. Grellier, C. Sergheraert, Synthesis and invitro and invivo antimalarial activity of N- (7-Chloro-4-quinolyl)-1,4-bis(3-aminopropyl)piperazine derivatives, J. Med. Chem. 46 (2003) 542–557.

[20] U. Ram Shankar, S. Neelima, J. Sanjay, K. Nawal, C. Ramesh, A. Sudershan, Optically Active antifungal azoles: synthesis and antifungal activity of (2R,3S)-2-(2,4- difluorophenyl)-3-(5-{2[4-aryl-piperazin-1-yl]-ethyl}-tetrazoll-2-yl/1-yl)-1-[1,2,4]- triazol-1-yl-butan-2-ol, Biorg.Med. Chem. 12 (2004) 2225–2238.

[21] M.X. Dong, L. Lu, H. Li, X. Wang, S. Jiang, Q.Y. Dai, Design, synthesis, and biological activity of novel 1,4-disubstituted piperidine/piperazine derivatives as CCR5 antagonist-based HIV-1 entry inhibitors, Bioorg. Med. Chem. Lett. 22 (9) (2012) 3284–3286.

[22] A. Foroumadi, S. Emami, A. Hassanzadeh, M. Rajaee, K. Sokhanvar, M.H. Moshafi, A. Shafiee, Synthesis and antibacterial activity of N-(5-benzylthio-1, 3, 4- thiadiazol-2-yl) and N-(5-benzyl sulfonyl-1, 3, 4-thiadiazol-2-yl) piperazinyl quinolone derivatives, Biorg. Med. Chem. Lett. 15 (20) (2005) 4488–4492.

[23] G.D. Abuo-Rehma, H.A. Sarhan, G.F.M. Gad, Design, synthesis, antibacterial activity and physicochemical parameters of novel N-4-piperazinyl derivatives of Norfloxacin, Bioorg. Med. Chem. 17 (2009) 3879–3886.

[24] S. Wang, X.D. Jia, M.L. Liu, Y. Lu, H.Y. Guo, Synthesis, antimycobacterial and antibacterial activity of ciprofloxacin derivatives containing a N-substituted benzyl moiety, Bioorg. Med. Chem. Lett. 22 (18) (2012) 5971–5975.

[25] a) L. Nagarapu, H.K. Gaikwad, K. Sirikonda, J. Mateti, R. Bantu, P.S. Raghu, K.M. Mahduri, S.V. Kalivendi, Synthesis and cytotoxicity evaluation of 1-[3-(9*H*- carbazol-4-yloxy)-2-hydroxypropyl]-3-aryl-1H-pyrazole-5-carboxylic acid derivatives, Eur. J. Med. Chem. 45 (2010) 4720–4725;
b) L. Nagarapu, J. Mateti, H.K. Gaikwad, R. Bantu, M. Sheebarani, N.J.P. Shubhasini, Synthesis and anti-inflammotory activity of some novel 3-phenyl-*N*-[3-(4-phenylpiperazin-1yl) propyl] 1*H*-pyrazole-5-carboxamide derivatives, Bioorg Med. Chem. Lett. 21 (2011) 4138–4140;
c) L. Nagarapu, S. Vanaparthi, R. Bantu, C.G. Kumar, Synthesis of noval benzo [4,5]thiazolo[1,2- *a*]pyrimidine-3-carboxylate derivatives and biological evaluation as potential anticancer agents, Eur. J. Med. Chem. 69 (2013) 817–822.

[26] Michael Goldbrunner, Günther Loidl, Thomas Polossek, Albrecht Mannschreck, Erwin von Angerer, Inhibition of tubulin polymerization by 5,6-Dihydroindolo[2,1- a]isoquinoline derivatives, J. Med. Chem. 40 (1997) 3524–3533.

[27] Yu-Hsun Chang, Mei-Hua Hsu, Sheng-Hung Wang, Li-Jiau Huang, Keduo Qian, Susan L. Morris-Natschke, Ernest Hamel, Sheng-Chu Kuo, Kuo-Hsiung Lee, Design and synthesis of 2-(3-benzo[b]thienyl)-6,7-methylenedioxyquinolin-4- one analogues as potent antitumor agents that inhibit tubulin assembly, J. Med. Chem. 52 (2009) 4883–4891.

[28] Romeo Romagnoli, Pier Giovanni Baraldi, Maria Kimatrai Salvador, Filippo Prencipe, Carlota Lopez-Cara, Santiago Schiaffino Ortega, Andrea Brancale, Ernest Hamel, Ignazio Castagliuolo, Stefania Mitola, Roberto Ronca, Roberta Bortolozzi, Elena Porcù, Giuseppe Basso, Giampietro Viola, Design, synthesis, *in vitro* and *in vivo* anticancer and anti-angiogenic activity of novel 3-Arylamino benzofuran derivatives targeting the colchicine site on tubulin, J. Med. Chem. 58 (2015) 3209–3222.

[29] B. Keerthana, J. Swathi Reddy, T. Saritha Jyostna, S. Sree Kanth, M. Vijjulatha, Design, synthesis, molecular docking and biological evaluation of new di-thiocarbamates substituted benzimidazole and chalcones as possible chemotherapeutic agents, Biorg. Med. Chem. Lett. 22 (2012) 3274–3277.

[30] L.L.C. Schrödinger, Glide, Version 5.6, 2010 (New York, NY).

[31] R.B. Ravelli, B. Gigant, P.A. Curmi, I. Jourdain, S. Lachkar, A. Sobel, M. Knossow, Insight into tubulin regulation from a complex with colchicines and a stathmin-like domain, Nature 428 (2004) 198–202.

[32] L.L.C. Schrodinger, Ligprep 2.0, 2010. New York, NY, USA.

[33] G.A. Kaminski, R.A. Friesner, J. Tirado-Rives, W.L. Jorgensen, Evaluation and reparametrization of the OPLSAA force field for proteins via comparison with accurate quantum chemical calculations on peptides, J. Phys. Chem. B 105 (28) (2001) 6474–6487.